Advances in Engineering Research : Possibilities and Challenges
ISSN Print: 3079-5192
ISSN Online: 3079-5206
https://doi.org/10.63313/AERpc.9037

Nonlinear dynamics analysis of shaft crack

Chengxiang Hu*. Fuhao Liu and Yanan Shi
Qingdao University of Technology, Qingdao 266000, China
Email: 1172579281@qq.com

How to cite this paper: Hu, C. X., Liu, F. H., & Shi, Y. N. (2025). Nonlinear dynamics analysis of shaft crack. Advances in Engineering Research: Possibilities and Challenges, 2(1), 58-65. ISSN Print: 3079-5192; ISSN Online: 3079-5206.
https://doi.org/10.63313/AERpc.9037
Published: 2025-07-24

Abstract

Considering the "breathing" phenomenon of cracks in a rotor system as the shaft rotates, this study derives the true breathing formula for shaft cracks, adopts more realistic flexural and torsional stiffnesses of the cracked shaft segments, and establishes a time-varying stiffness matrix for the cracked shaft. Subse-quently, a finite element dynamics model of the gear transmission system con-taining gear-shaft-bearing is established to elucidate the dynamic characteristics of the system affected by the shaft crack. The dynamic characteristics of the sys-tem un-der the influence of shaft cracks are analyzed by changing the crack pa-rameters such as different crack depths and different numbers of cracks.

Keywords

Shaft crack; nonlinear dynamics; dynamic response

1. Introduction

Rotating machinery is one of the most important mechanical equipment in modern industrial society, and various rotor power systems have a wide range of applications in power generation, aircraft engines, compressors, pumps and many other industrial fields. As the most common failure mode of rotor systems, it is of great significance to accurately establish the physical model of the cracked unit and analyze the vibration characteristics of the crack under different failure sources for fault localization and diagnosis.[1]

Mayes[2] proposed a cosine model to simulate the crack opening and closing laws. On this basis, Wen[3] developed a breathing model to simulate the crack opening and closing. Patel[4] investigated the effect of crack breathing effect on its vibration characteristics. A1-shudeifat[5] considered the time-varying product of the inertia of the cracked cross-section and the rotational inertia, so as to derive a new stiffness model of the cracked rotor, and the experimental model was verified.[6]

Based on the combination of theoretical derivation and finite element numerical simulation, we analyze and study the influence mechanism of the shaft crack on the rotor-bearing system, use more accurate crack modeling that simulates the real situation, establish a model of the gear-rotor-bearing system under the influence of the shaft crack, and accurately analyze the "respiratory" time-varying characteristics and the "respiration" of the flexural and torsional stiffnesses of the cracked shaft section of the rotor in the rotor system. The time-varying characteristics of the cracked rotor shaft segment in the rotor system and the dynamic characteristics of the system when the shaft crack occurs are precisely analyzed, and the effects of the shaft crack failure on the system are explored by changing the parameters such as different crack depths and different crack locations.

2. Model And Methodology

2.1. Spur gear system dynamics modeling

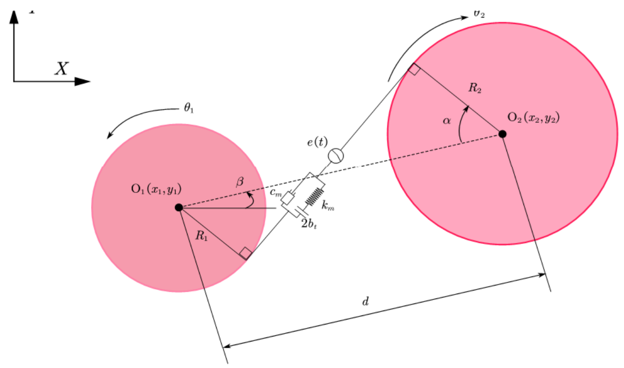

Fig 1. Nonlinear dynamic model for the gear pair.

Fig 1describes the generalized coordinates of the paired gears. The motion of the gear set can be defined in terms of six generalized coordinates to define the motions of the gear sets which are assumed to be planar motions, two translation coordinates and one rotation coordinate for each gear coordinates. The dotted and solid circles represent the gear sets before and after the movements, respectively.

The axis centers of the static gears are denoted by points O_1, O_2. $L_0 = R_1 + R_2$, R_1 and R_2 denote the pitch circle radius of the pinion and gear, respectively Considering gear translational motions, the axis centers can move to points O_8' and O_{18}', respectively. Here, two static coordinate systems $o_i\ x_i\ \ y_i$ (i = 1, 2) are established on the axis centers O_1 and O_2, respectively. The angle β represents the position of the gear relative to the pinion after motion. Gi represents the mass center of gear i. ϕ_{01} and ϕ_{02} are the initial eccentricity angles. For simplicity, they are generally assumed to be zeroes at t = 0 s.

The vibration displacements of gear i are given by translational coordinal x_i and y_i. The rotation angle displacements of gear i are given by angular coordinates, ϕ_1 and ϕ_2, which can be expressed as follows:

$$\phi_1(t) = \theta_1(t) + \varphi_1, \phi_2(t) = \theta_2(t) + \varphi_2 \tag{1}$$

where, θ_i is the torsional angle displacement superimposed on the rigid-body rotation of gear i.

Let the rotation direction of pinion is positive, then the displacement vectors of the mass centers G1, G2 in the coordinate systems $o_1x_1y_1$, $o_2x_2y_2$ can be expressed as, respectively.

$$\boldsymbol{r}_1 = x_1\boldsymbol{i} + \mathrm{y}_1\boldsymbol{j}, \boldsymbol{r}_2 = x_2\boldsymbol{i} + \mathrm{y}_2\boldsymbol{j} \tag{2}$$

where, i and j are unit vectors along the x and y axes, respectively.

Due to the translational motions of pinion and gear, the gear center distance d_0 is changed to d after the motion. The actual center distance d is given by

$$L = \sqrt{\left(x_2 - x_1 + L_0 \cos a_0\right)^2 + \left(y_2 - y_1 + L_0 \sin a_0\right)^2} \tag{3}$$

The position angle β can be expressed as:

$$\beta = \tan^{-1} \frac{y_2 - y_1 + L_0 \sin a_0}{x_2 - x_1 + L_0 \cos a_0} \tag{4}$$

Fig 1shows a nonlinear dynamic model for the gear pair at any mesh position after motion. The gear mesh is represented as a pair of rigid disks connected by a spring damper set along the LOA. The LOA is defined as the common tangent line of the base circles in the gear set having involute profiles. The actual pressure angle α is defined as the angle between the LOA and the direction of velocity at the pitch point, and can be expressed as:

$$\alpha = \cos^{-1} \frac{R_2 + R_1}{L} \tag{5}$$

It can be seen from Eqs. (4) and (5) that the gear position angle and pressure angle are affected by the translational motions of the gears while the previous studies nearly neglected these effects.

The change of gear center distance will also lead to the change of the gear contact ratio, according to the definition of the contact ratio, the actual contact ratio m_p can be given by

$$m_p = \frac{\sqrt{R_{a1}^2 - R_1^2} + \sqrt{R_{a2}^2 - R_2^2} - L\sin\alpha}{P_b} \tag{6}$$

here $R_{a1}$and R_{a2} are the radii of the addendum circles for pinion and gear, and p_b is the base pitch.

The relative displacement of the dynamic transmission error $\delta(t)$ along LOA can be expressed as:

$$\delta(t) = (x_1 - x_2)\sin(\alpha - \beta) + (y_1 - y_2)\cos(\alpha - \beta) + R_1\theta_1 + R_2\theta_2 \tag{7}$$

where, θ_6 is the angular displacement of the pinion, θ_{16} is the angular displacement of the large gear.

Based on the theory of viscoelasticity, the dynamic mesh force (DMF) consists of elastic force and damping force along the LOA and can be written as:

$$F_{\mathrm{m}} = k_m f\left(\delta, b_t\right) + c_m f_1\left(\delta, b_t\right) \tag{8}$$

where, k_m and c_m are time-varying mesh stiffness and damping, $c_m = 2\xi_m\sqrt{k_m J_1 J_2/(J_2 R_1^2 + J_1 R_2^2)}$, ξ_m is the damping ratio (0.030.17); b_t is time-varying half gear backlash. $f(\delta, b_t)$ and $f_1(\delta, b_t)$ are the nonlinear functions for backlash and relative speed respectively and can be expressed as:

$$f\left(\delta, b_t\right) = \begin{cases} \delta - \mathrm{sign}\left(\delta\right) b_t & \left|\delta\right| > b_t \\ 0 & else \end{cases} \tag{9}$$

$$f_1\left(\delta, b_t\right) = \begin{cases} \dot{\delta} - \mathrm{sign}\left(\delta\right) \dot{b}_t & \left|\delta\right| > b_t \\ 0 & else \end{cases} \tag{10}$$

2.2. Modelling of the Shaft Crack

During the operation of the gear train, the stiffness of the cracked shaft element changes with rotation due to gravity and rotational motion. When the crack is closed, the cracked shaft unit stiffness is approximately the same as the normal shaft stiffness. When the crack is in the fully open state, the cracked shaft unit is damaged the most and the stiffness is the minimum value. During shaft rotation, the crack is more in the half-open, half-closed transition state. During this period, the amount of stiffness reduction varies continuously with time. In order to accurately understand the concept of crack breathing behavior, Fig 2 shows various states of transverse breathing cracks during shaft rotation. In view of the time-varying stiffness of the cracked shaft element, a cosine model is used to simulate the crack opening and closing pattern.

$$f\left(t\right) = \frac{\left(1 + \cos\left(\Omega t\right)\right)}{2} \tag{11}$$

Here Ω is defined the rotational speed of the rotor in radians per second, and N is the rotational speed of the rotor in revolutions per minute.
The stiffness of crack shaft element can be expressed as

$$K_c\left(t\right) = K_e - f\left(t\right) K_c^d \tag{12}$$

where $K_c(t)$ is the time-varying stiffness matrix of the crack shaft element, and K_c^d is the stiffness reduction amount of the crack shaft element.

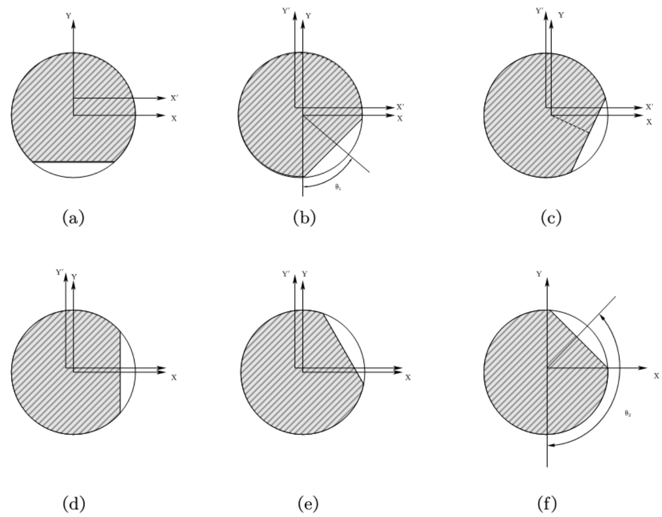

Fig 2. Different states of transverse breathing crack during shaft rotation

The schematic diagram of crack section is shown in Fig 3, and the shaded part indicates the cracked part. *O-vw* is the fixed coordinate system with the original center of the shaft as the coordinate origin, where the coordinate origin *O* is the centroid of the section of the shaft without crack, $O' - v'w'$ is the fixed coordinate system with the new centroid of the shaft after crack as the coordinate origin, and O' is the centroid of the eccentric section of the crack. αo is the circumferential angle of the crack, *e* is the eccentricity of the crack cross section relative to the original centroid, *h* is the crack depth, *r* is the radius of the rotating shaft, and the dimensionless crack depth $\lambda_s = h/2r$.

A_c represents the area of the crack section, and the area of the area of the crack-free section is A_r

$$A_r = \pi r^2 - \left(r^2 2\alpha_1 - \sqrt{2rh - h^2}\left(r - h\right)\right) \quad \mathrm{r>h} \tag{13}$$

When $r > h$, $\alpha_0 = 2\alpha_1$, $\alpha_1 = arctan(\sqrt{2rh - h^2}/2r - h)$

The eccentricity of the crack section is

$$e = \frac{1}{A_r}\int_{-r}^{r-h} 2yxdy\,, e = \frac{2r^3}{3A_r}\left(\frac{2hr - h^2}{r^2}\right) \tag{14}$$

As the crack propagates, the moment of inertia and the moment of polar inertia of the crack part also change. The moment of inertia of the crack part to the coordinate axis and to the origin of the fixed coordinate system are expressed as follows

$$I_v^O = 2\int_{r-h}^{r} w^2\sqrt{r^2 - w^2}\,dw \tag{15}$$

$$I_w^O = 2\int_0^{\sqrt{2rh-h^2}} v^2\left(\sqrt{r^2 - v^2} - r + h\right)dv \quad \mathrm{r>h} \tag{16}$$

$$I_p^O = I_v^O + I_w^O \tag{17}$$

Use the Simpson formula to convert the above integral formula as follows

$$I_v^O = \frac{h}{3}\left[\sqrt{2hr-h^2}\,(r-h)^2 + \frac{1}{2}\sqrt{4hr-h^2}\,(2r-h)^2\right] \tag{18}$$

$$I_w^O = \frac{\left(2hr-h^2\right)^{\frac{3}{2}}}{3}\left[\frac{1}{2}\sqrt{4r^2-2hr+h^2}-r+h\right] \quad \text{r>h} \tag{19}$$

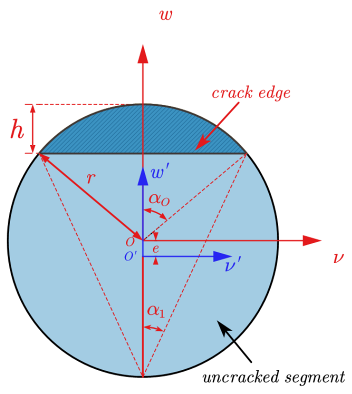

(a)

Fig 3. Schematic diagram of the cracked element cross section.

Considering the effect of the crack on the centroid, combined with the parallel shift axis theorem, the moments of w0 of the crack part on the coordinate axes O

$$I_{v'}^{O'} = I_v^O + A_r e^2, I_{w'}^{O'} = I_w^O \tag{20}$$

$$I_{p'}^{O'} = I_{v'}^{O'} + I_{w'}^{O'} \tag{21}$$

Therefore, the crack element stiffness matrix reduction is expressed as (21), G represents 80 Gpa for shear modulus, E is 210 Gpa for elastic modulus and ξ is 4/3 for shear coefficient.

The time-varying stiffness matrix Kc(t) of cracked shaft element can be obtained by substituting stiffness reduction element K_c^d into formula (13).

$$K_c^d = \begin{bmatrix} \frac{12EI_{v'}^{O'}}{l^3} & 0 & 0 \\ 0 & \frac{12EI_{w'}^{O'}}{l^3} & 0 \\ 0 & 0 & \frac{GI_{p'}^{O'}}{l} \end{bmatrix} \tag{22}$$

3. The influence of eccentricity on the system

In the manufacturing process of gears, due to machining or casting, crack failures can occur as the shaft rotates.[7] The effect of different shaft cracks on the dynamic response of the gear system is studied and compared on the basis of considering the constant bearing stiffness.

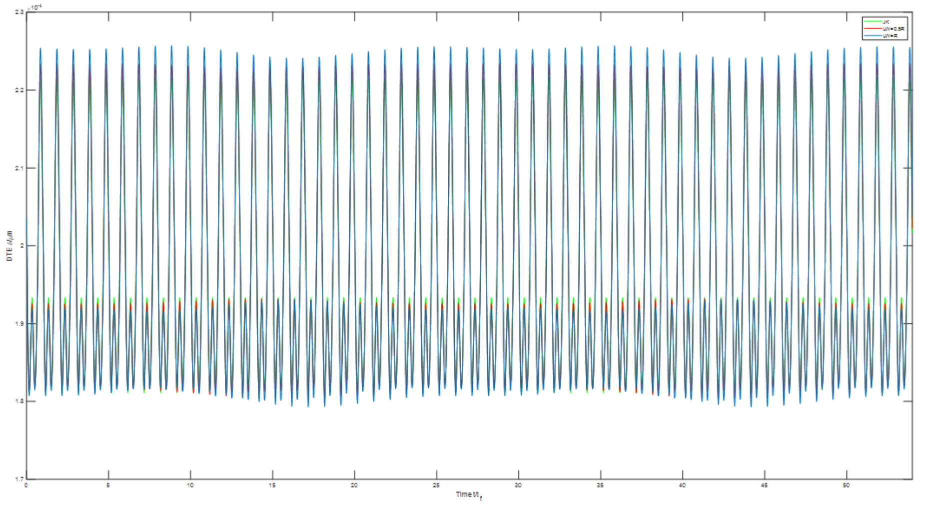

Fig 4 . Dynamic response at different crack depths

The results of the vibration response of the system with different crack depths are shown in Fig 4. In this part, the time course diagram of DTE is utilized to study the effect of shaft cracks on the dynamic response of the gear system. The crack depths of the cracked units on the drive shaft are set to 0.151 and 0.302 mm, i.e., half of the shaft radius and circumferential radius, respectively. Compared to the normal gear shaft system without faults, it can be observed that when the crack depth on the shaft is zero, the system DTE is a stable periodic motion. When the crack failure on the shaft is considered, it is found that the dynamic response of the system fluctuates, which is due to the change in the stiffness matrix of the shaft unit and the decrease in the local stiffness of the crack, which in turn affects the dynamic response of the gear system. The dynamic transmission error curves show large oscillations, but the two curves have the same rule of change. The amplitude and magnitude of the periodic fluctuations of DTE increase with the increase of eccentricity, but the fluctuation trend is basically the same.

4. Conclusion

The effect of cracks on the shaft on the gear system is considered. The most commonly used three-degree-of-freedom typical dynamic model of was established, and the dynamic equations of the system were given according to Newton's second law. The results show that when the crack depth on the shaft is zero, i.e., the shaft is normal, the DTE of the system is a stable periodic motion. When crack failure is considered, due to local stiffness change in the shaft unit, stiffness change during the engagement cycle leads to fluctuation in the dynamic response of the system. As the depth of the crack on the shaft increases, the amplitude and magnitude of the DTE cycle fluctuations become larger, but the fluctuation trend is basically the same.

References

[1] Sabnavi, G., Kirk, R.G., Kasarda, M., Quinn, D.: Cracked shaft detection and diagnostics: a literature review. Shock Vib. Dig. 36(4), 287–297 (2004)

[2] Gasch, R.: A survey of the dynamic behaviour of a simple rotating shaft with a transverse crack. J. Sound Vib. 160(2),313–332 (1993)

[3] I. W. Mayes and W. G. R. Davies, "Analysis of the response of a multi-rotor-bearing system containing a transverse crack in a rotor," J. Vib. Acoust. Stress Rel. Des., vol. 106, no. 1, p. 139, 1984.

[4] O. S. Jun, H. J. Eun, Y. Y. Earmme, and C.-W. Lee, "Modelling and vibration analysis of a simple rotor with a breathing crack," J. Sound Vib,vol. 155, no. 2, pp. 273–290, Jun. 1992.

[5] J. M. Gao and X. M. Zhu, "Research on the breathing model of crack on rotating shaft," Chin. J. Appl. Mech., vol. 9, no. 1, pp. 108–112,1992.

[6] M. A. AL-Shudeifat, "On the finite element modeling of the asym-metric cracked rotor," J. Sound Vib., vol. 332, no. 11, pp. 2795–2807, May 2013.

[7] M. A. Al-Shudeifat and E. A. Butcher, "New breathing functions for the transverse breathing crack of the cracked rotor system: Approach for critical and subcritical harmonic analysis," J. Sound Vib., vol. 330, no. 3, pp. 526–544, Jan. 2011.